

# Metal isotope and density functional study of the tetracarboxylatodicopper(II) core vibrations

Piotr Drożdżewski\*, Anna Brożyna

*Institute of Inorganic Chemistry and Metallurgy of Rare Elements, Faculty of Chemistry, Wrocław University of Technology,  
Wybrzeże St. Wyspiańskiego 27, 50-370 Wrocław, Poland*

Received 14 December 2004; received in revised form 22 February 2005; accepted 22 February 2005

## Abstract

Vibrational spectra of tetrakis(acetato)diaquadicopper(II) complex have been deeply examined in order to provide a detailed description of dynamics of  $[\text{Cu}_2\text{O}_8\text{C}_4]$  core being a typical structural unit of most copper(II) carboxylates. Low frequency bands related to significant motions of metal atoms were detected by metal isotope substitution. Observed spectra and isotope shifts were reproduced in DFT calculations. For clear presentation of computed normal vibrations, a  $D_{4h}$  symmetry approximation was successfully applied. Basing on observed isotope shifts and calculation results, all skeletal vibrations have been analyzed including normal mode with the largest Cu...Cu stretching amplitude assigned to Raman band at  $178\text{ cm}^{-1}$ .

© 2005 Elsevier B.V. All rights reserved.

**Keywords:** Copper(II) carboxylates; IR and Raman spectra; Normal vibrations; DFT calculations

## 1. Introduction

A variety of polynuclear metal carboxylates have been prepared and investigated so far with special attention placed on possible metal–metal interactions. Large group of these compounds consists of copper(II) complexes with the formula  $[\text{Cu}_2(\text{OOCR})_4(\text{L})_2]$  (R: organic group, L: Lewis base) containing the characteristic  $[\text{Cu}_2\text{O}_8\text{C}_4]$  core. In most cases, these compounds were investigated by X-ray diffraction method accompanied by magnetic and selected spectroscopic measurements [1]. However, the majority of vibrational attempts were limited to discussion of the carboxylate group vibrations. Much less work was done on  $[\text{Cu}_2\text{O}_8\text{C}_4]$  core vibrations absorbing in the far-IR region. Lever and Ramaswamy [2] have investigated this problem for several copper(II) carboxylates, employing the deuteration,  $^{65}\text{Cu}$  isotope substitution and low temperature techniques. Based on those experiments, several bands located between 200 and  $450\text{ cm}^{-1}$  were pointed out as being generated by Cu–O

vibrations, but without more precise characterization. Only two Cu–O stretching vibrations have been proposed by Fani-ran and Patel [3] for copper complexes with acetic acid and its chloro-derivatives. These bands were found at about 330 and  $370\text{ cm}^{-1}$ . At similar frequency ( $334\text{ cm}^{-1}$ ), the anti-symmetric Cu–O stretching vibration was postulated for copper(II)-*N*-acetyl- $\beta$ -alaninato complex [4]. The vibrations of water molecules, frequently present in the metal acetates, were studied by Baraldi and Fabbri [5]. However, only a general statement was made that bands observed below  $450\text{ cm}^{-1}$  refer to metal–oxygen vibrations, without distinguishing the metal–water modes. Metal–metal interactions were studied by Raman spectroscopy for Re, Mo, Rh, Ru, Fe and Cu complexes [6]. For Rh and Cu acetates, the transitions at about  $170\text{ cm}^{-1}$  were postulated as  $\nu(\text{M}–\text{M})$  vibrations, but this assignment was not unambiguous. In another work [7], the excitation profiles of 700 and  $320\text{ cm}^{-1}$  Raman bands of copper(II) acetate were measured in order to characterize the electronic transitions of this compound.

As results from the above review, the vibrations of  $[\text{Cu}_2\text{O}_8\text{C}_4]$  core are not completely localized and characterized. Among eight expected Cu–O stretching vibrations

\* Corresponding author. Tel.: +48 71 3203909; fax: +48 71 3284330.  
E-mail address: [piotr.drozdzewski@pwr.wroc.pl](mailto:piotr.drozdzewski@pwr.wroc.pl) (P. Drożdżewski).

(some may be degenerate) only two, anti-symmetric were assigned so far. The discussed  $[\text{Cu}_2\text{O}_8\text{C}_4]$  group must also show several O–Cu–O bending modes coupled to a varying extent with Cu–O–C and O–C–O vibrations as well as with some Cu–O stretching ones. It is difficult to analyze such a complicated system only in an empirical way. Thus, the theoretical predictions will be very helpful in this matter.

In the present work, the far-IR region vibrations of the  $[\text{Cu}_2\text{O}_8\text{C}_4]$  system were elaborated with help of the  $^{63}\text{Cu}$ – $^{65}\text{Cu}$  isotope replacement and quantum calculations on the density functional theory (DFT) level. The experiments and calculations were performed for copper(II) acetate monohydrate, a relatively simple molecule containing the typical  $[\text{Cu}_2\text{O}_8\text{C}_4]$  dinuclear unit.

## 2. Experimental

### 2.1. Preparation of the complexes

The copper(II) acetate monohydrate was prepared by treating a light excess of freshly precipitated copper hydroxide with aqueous solution of the acetic acid. The isotopically labeled complexes were obtained on the same way, but on the 0.1 mmole scale. The deuterated compound was prepared by three-fold re-crystallization from  $\text{D}_2\text{O}$ .

### 2.2. Physical measurements

The far-IR spectra were recorded with  $0.5\text{ cm}^{-1}$  resolution on a Fourier-Transform PE 2000 spectrometer with samples as Nujol mulls between polyethylene plates. For the middle-IR region, a FTIR 1600 instrument and KBr disc technique were used. Raman spectra were collected with the right angle optics configuration on a Jobin-Yvon T64000 spectrophotometer using the 514.5 nm Ar–Kr laser excitation.

### 2.3. Computations

Quantum calculations on DFT level were performed using GAUSSIAN98 package [8]. The Becke's three-parameter hybrid functional B3LYP [9] and LanL2DZ basis [10,11] augmented with d-polarization functions on heavy atoms were applied. The vibrational frequencies and intensities were calculated using the energy-minimized structure and harmonic approximation. The potential energy distribution was calculated by Balga programs written by Lapinski and Nowak [12]. Molecule drawing and theoretical spectra were prepared with help of Molden [13] and Animol [14] applications. Before plotting the theoretical Raman spectrum, the computed intensities were corrected for  $\nu^4$  and Boltzman distribution factors [15].

Table 1

Selection of optimized and measured structural parameters ( $\text{Å}$ ,  $^\circ$ ) of the tetrakis(acetato)diaquadicopper(II) skeleton

Parameter	Optimized	Observed	
		[17]	[18]
Cu1–Cu5	2.610	2.616(1)	2.614(2)
Cu1–O2	2.001	1.950(3)	1.952(2)
Cu5–O4	2.032	1.945(4)	1.941(2)
Cu1–O9	2.030	1.994(3)	1.992(1)
Cu5–O11	2.001	1.986(3)	1.990(1)
Cu1–O31	2.305	2.156(4)	2.161(2)
C3–O2	1.266	1.248(6)	1.261(2)
C3–O4	1.271	1.274(7)	1.259(2)
C10–O9	1.271	1.268(6)	1.261(2)
C10–O11	1.266	1.251(6)	1.256(2)
C3–C15	1.527	1.506(7)	1.502(2)
C10–C17	1.527	1.495(5)	1.500(2)
O2–Cu1–Cu5	85.6	–	82.8(1)
O4–Cu5–Cu1	84.7	–	86.1(1)
O9–Cu1–Cu5	84.5	–	82.7(1)
O11–Cu5–Cu1	85.8	–	86.1(1)
O2–Cu1–O9	89.7	89.1(1)	89.2(1)
O4–Cu5–O11	89.6	91.1(1)	87.4(1)
Cu1–O2–C3	121.6	124.9(4)	124.5(1)
Cu5–O4–C3	121.1	120.7(3)	121.2(1)
Cu1–O9–C10	121.3	124.9(3)	125.2(1)
Cu5–O11–C10	121.4	121.9(3)	121.4(1)
O2–C3–O4	127.0	125.4(5)	125.3(1)
O9–C10–O11	127.0	124.2(4)	124.4(1)
O2–C3–C15	116.9	118.8(5)	117.5(1)
O9–C10–C17	116.2	117.0(4)	117.4(1)
O31–Cu1–O2	106.0	93.3(2)	93.5(1)
O31–Cu1–O9	83.7	97.7(2)	93.1(1)

## 3. Results and discussion

### 3.1. Far-IR region

For the theoretical study of the  $[\text{Cu}_2\text{O}_8\text{C}_4]$  vibrations, the complete molecule of  $[\text{Cu}_2(\text{OOCCH}_3)_4(\text{H}_2\text{O})_2]$  has been chosen. The simplest model, like copper formate was rejected because the nature of the atom (hydrogen or carbon) directly bonded to carboxylate carbon significantly influences the metal-carboxylate group vibrations, as has been demonstrated before [16]. Thus, the results obtained for copper acetate are much better compared with respective data of similar complexes containing the variously substituted carboxylates as bridging ligands.

The initial structural parameters were taken from the X-ray [17] and neutron [18] diffraction analysis of copper acetate monohydrate. The geometry optimization was performed under relaxation of all internal degrees of freedom. A selection of optimized, skeletal parameters is listed in Table 1 and compared with the respective data observed. The computed molecular structure together with atom numbering system is presented in Fig. 1. Despite the very symmetric appearance of the  $[\text{Cu}_2(\text{OOCCH}_3)_4(\text{H}_2\text{O})_2]$  molecule, its real symmetry is  $C_i$  because acetate bridges are not structurally the same. The largest differences are observed for the Cu–O bond

lengths, which are related to intermolecular hydrogen bonding in which only one pair of opposite carboxylate groups is involved [18]. These differences are approximately twice as small as in the optimized structure. The Cu–O distances are slightly overestimated, but their relative lengths differ less than 1.5%. Among the skeletal angles, the largest differences concern the location of water molecules, which are more displaced from the Cu···Cu line in the optimized structure than in the real molecules.

Basing on the optimized structure, the harmonic vibrational frequencies, IR intensities and Raman activities were subsequently calculated using the numerical differentiation of analytical gradients. All frequencies were positive, confirming that the optimized structure corresponds to the potential energy minimum. The theoretical spectra produced from the calculated data are presented in Fig. 2, together with the observed ones. For the detection of the metal–ligand vibrations, the isotope effects due to  $^{63}\text{Cu}$ – $^{65}\text{Cu}$  replacements were measured and computed. The resulting wavenumber downshifts, listed in Fig. 2 by band maxima, are very useful in proper attribution of computed normal vibrations to observed IR and Raman transitions. The largest isotope shifts

are observed for two IR bands at 376 and 331  $\text{cm}^{-1}$ . Similar shifts were computed for closely positioned bands at 344 and 341  $\text{cm}^{-1}$ . Two lower frequency bands showing the 1.0 and 0.5  $\text{cm}^{-1}$  isotope shifts were correlated with two theoretical transitions exhibiting the 1.0 and 0.6  $\text{cm}^{-1}$  shifts and well corresponding intensities. In the Raman spectrum, the 2.0  $\text{cm}^{-1}$  shift was detected only for one band at 178  $\text{cm}^{-1}$ . This effect indicates that the band calculated at 168  $\text{cm}^{-1}$  (1.2  $\text{cm}^{-1}$  shift) is the best candidate for the corresponding mode. A smaller, 0.5  $\text{cm}^{-1}$  displacement was observed for the 253  $\text{cm}^{-1}$  band correlated with Raman active transitions computed at similar frequencies. The discrepancies in the observed and calculated shifts are partially due to the shape of several Raman bands being worse than observed in the IR spectrum. In all spectra, the remaining bands were correlated on the basis of their similar frequencies and intensities.

In order to get a better insight into vibrational character of presented transitions, the potential energy distribution (PED) terms were calculated for all normal modes of  $[\text{Cu}_2(\text{OOCCH}_3)_4(\text{H}_2\text{O})_2]$  molecule. For this purpose, a complete set of 102 symmetrized internal coordinates was constructed. Since for metal carboxylates, like this presented

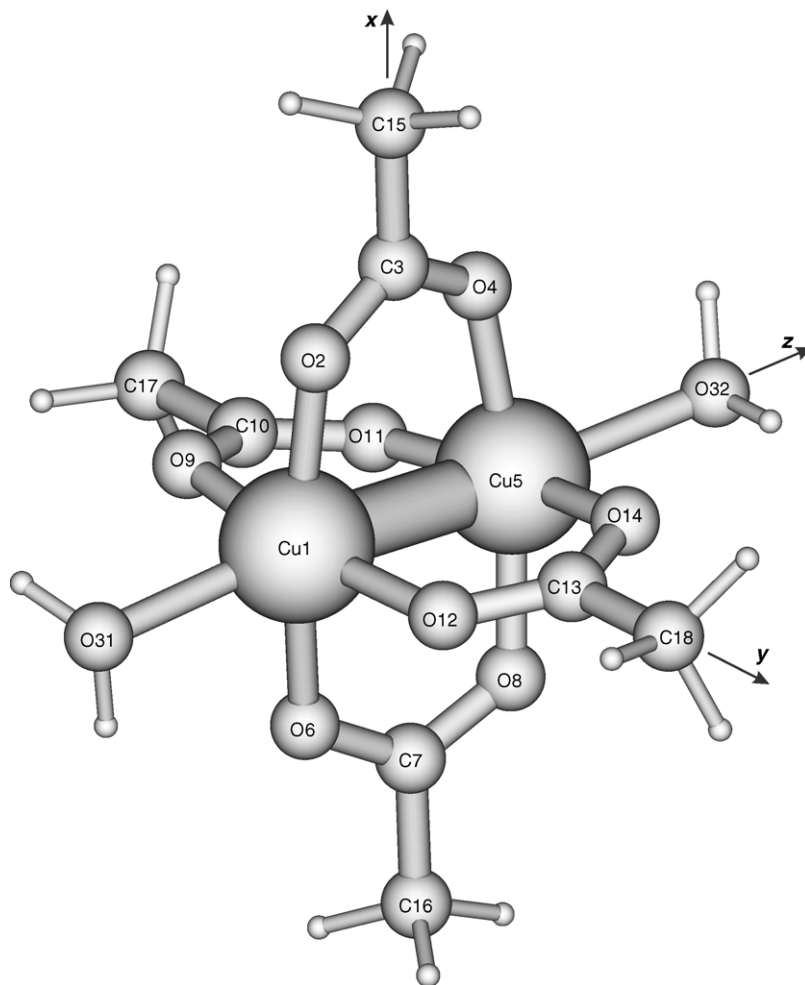


Fig. 1. Computational model of the  $[\text{Cu}_2(\text{OOCCH}_3)_4(\text{H}_2\text{O})_2]$  complex.

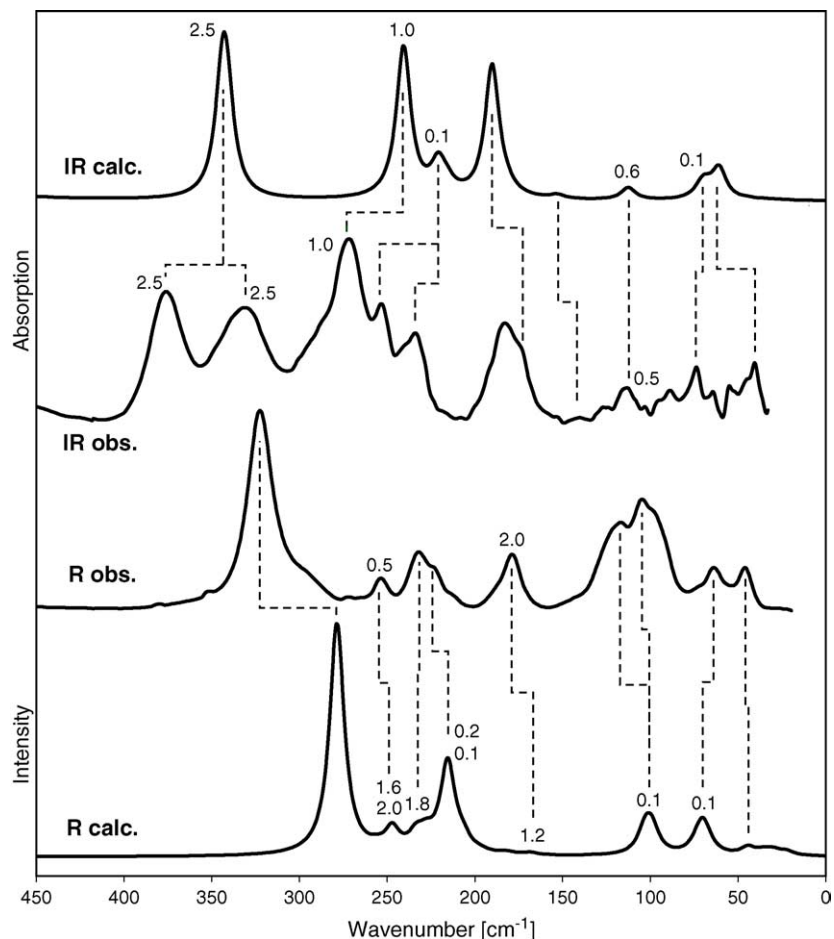


Fig. 2. Observed and DFT calculated spectra in far-IR region.

here, one of the most interesting problems is the metal–metal interaction, the respective Cu–Cu stretching coordinate has been implemented. As a result, the five-membered Cu–O–C–O–Cu rings appear and their bending coordinates could be defined as recommended by Pulay et al. [19]. The most significant atom displacements have been presented for these coordinates in Fig. 3. Pulay's recommendations were also used for methyl group coordinates. Several attempts were made for the symmetry of  $[\text{Cu}_2(\text{OCC})_4]$  skeletal coordinates starting from simple  $C_i$  up to  $D_{4h}$  symmetry. Calculated PED characterizations of the respective normal vibrations were the simplest and the most clear for the  $D_{4h}$  symmetry. For lower symmetry, most of the skeletal vibrations were described as the sums of several PED terms of comparable contributions. Therefore, taking into account that the real and calculated structure of the  $[\text{Cu}_2(\text{OCC})_4]$  skeleton only slightly deviate from  $D_{4h}$  symmetry, it was decided to use the  $D_{4h}$  symmetry as a good approximation for the clear presentation of calculated  $[\text{Cu}_2(\text{OCC})_4]$  skeletal vibrations. A small disadvantage of this approximation is that the mutual exclusion rule is not exactly valid. Some of the calculated u type vibrations, besides the expected significant IR intensity,

show also small Raman activity. The reverse phenomenon is noticed for g modes. Also the  $A_{2g}$ ,  $A_{1u}$ ,  $B_{1u}$  and  $B_{2u}$  modes, which are not active at all for ideal  $D_{4h}$  symmetry, here have appeared as very weak transitions. The coordinates related to the water molecules were treated under the  $C_i$  symmetry. The results of the above procedure have been presented in Table 2.

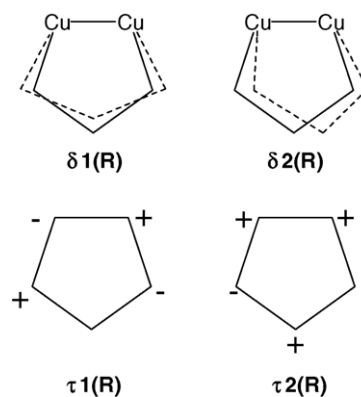


Fig. 3. Atom displacements in deformations of five-membered ring. Plus and minus represent the atom displacements out of the ring plane.

Table 2

Selected normal vibrations of tetrakis(acetato)diaquadicopper(II) complex, representing the dynamics of the  $[\text{Cu}_2(\text{OOC})_4]$  core ( $D_{4h}$ ) and some  $\text{H}_2\text{O}$  related modes ( $C_i$ )

Species		Observed ( $\text{cm}^{-1}$ )		Calculated ( $\text{cm}^{-1}$ )		Assignment <sup>a</sup> PED(%)
$D_{4h}$	$C_i$	IR	R	IR	R	
$E_g$			1535		1584	$\nu(\text{C—O})$ -82
$B_{2u}$		1620 <sub>sh</sub>		1551		$\nu(\text{C—O})$ -84
$A_{2u}$		1605		1530		$\nu(\text{C—O})$ -84
$A_{1g}$			1444		1422	$\nu(\text{C—O})$ -64 + $\nu(\text{C—C})$ -18
$E_u$		1421		1414		$\nu(\text{C—O})$ -65 + $\nu(\text{C—C})$ -14
$B_{1g}$			1426		1404	$\nu(\text{C—O})$ -57 + $\nu(\text{C—C})$ -18
$A_{1g}$			951		958	$\nu(\text{C—C})$ -47 + $\nu(\text{C—O})$ -26 + $\delta_1(\text{R})$ -24
$E_u$		944		950		$\nu(\text{C—C})$ -41 + $\nu(\text{C—O})$ -20 + $\delta_1(\text{R})$ -17
$B_{1g}$			951		947	$\nu(\text{C—C})$ -50 + $\nu(\text{C—O})$ -25 + $\delta_1(\text{R})$ -22
$A_{1g}$			692		689	$\delta_1(\text{R})$ -62 + $\nu(\text{C—C})$ -28
$E_u$		692		678		$\delta_1(\text{R})$ -58 + $\nu(\text{C—C})$ -22
$B_{1g}$			706		671	$\delta_1(\text{R})$ -64 + $\nu(\text{C—C})$ -25
$B_{2g}$			635		637	$\tau_2(\text{R})$ -59
$E_u$		629		633		$\tau_2(\text{R})$ -63
$A_{2g}$			n.o.		623	$\tau_2(\text{R})$ -71
$E_g$			530		535 (0.5)	$\delta(\text{O—C—C})$ -43 + $\nu(\text{Cu—O})$ -34
$A_{2u}$		n.o. <sup>b</sup>		520		$\delta(\text{O—C—C})$ -57 + $\nu(\text{Cu—O})$ -28
$B_{2u}$		n.o.		482		$\delta(\text{O—C—C})$ -71 + $\nu(\text{Cu—O})$ -16
$E_u$		376 (2.5) <sup>c</sup>		344 (2.5)		$\nu(\text{Cu—O})$ -85
		331 (2.5)		341 (2.5)		
$A_{1g}$			323		279	$\nu(\text{Cu—O})$ -85
	$A_g$		253 (0.5)		256 (2.0)	$\nu(\text{Cu—OH}_2)$ -46 + $\nu(\text{Cu—O})$ -26 + $\delta(\text{O—C—C})$ -18
$E_g$			253 (0.5)		247 (1.6)	$\nu(\text{Cu—O})$ -51 + $\delta(\text{O—C—C})$ -32
			232		233 (1.8)	$\nu(\text{Cu—O})$ -31 + $\nu(\text{Cu—OH}_2)$ -28 + $\delta(\text{O—C—C})$ -17
$A_{2u}$		272 (1.0)		241 (1.0)		$\delta_2(\text{R})$ -58 + $\delta(\text{O—C—C})$ -18 + $\nu(\text{Cu—O})$ -12
$B_{2g}$			(232)		228	$\delta(\text{R—R}')$ -65 + $\tau(\text{Cu—O—C—C})$ -36
$B_{1u}$		n.o.		223 (0.1)		$\nu(\text{Cu—OH}_2)$ -41 + $\tau_1(\text{R})$ -39
$E_u$		253		221		$\tau(\text{R—R}')$ -43 + $\tau(\text{Cu—O—C—C})$ -27
		234		220		
	$A_u$	232		216 (0.1)		$\nu(\text{Cu—OH}_2)$ -42 + $\tau(\text{R—R}')$ -13
$B_{1g}$			224 <sub>sh</sub>		215 (0.2)	$\nu(\text{Cu—O})$ -78
$E_g$			210 <sub>sh</sub>		207	$\tau_1(\text{R})$ -41 + $\tau(\text{H}_2\text{O})$ -32
					197 (0.3)	$\tau_1(\text{R})$ -81 + $\delta_2(\text{R})$ -13
	$A_u$	175 <sub>sh</sub>		190		$\tau(\text{H}_2\text{O})$ -80
	$A_g$		n.o.		182 (0.3)	$\tau(\text{H}_2\text{O})$ -57 + $\tau_1(\text{R})$ -29
$A_{1g}$			178 (2.0)		168 (1.2)	$\nu(\text{Cu—Cu})$ -75 + $\nu(\text{Cu—OH}_2)$ -22
$B_{2u}$		140		153		$\delta_2(\text{R})$ -45 + $\nu(\text{Cu—O})$ -40 + $\delta(\text{O—C—C})$ -15
$A_{2g}$			n.o.		132	$\tau(\text{Cu—O—C—C})$ -81 + $\tau_2(\text{R})$ -12
$A_{2u}$		114 (0.5)		113 (0.6)		$\nu(\text{Cu—O})$ -58 + $\delta_2(\text{R})$ -28 + $\delta(\text{O—C—C})$ -16
$E_g$			117		103 (0.1)	$\delta_2(\text{R})$ -59 + $\delta_1(\text{O—Cu—OH}_2)$ -25
			105		99 (0.1)	$\delta_2(\text{R})$ -62 + $\delta_2(\text{O—Cu—OH}_2)$ -18 + $\tau_1(\text{R})$ -14
$B_{2u}$		n.o.		78		$\delta_2(\text{O—Cu—OH}_2)$ -47 + $\delta_2(\text{R})$ -27 + $\nu(\text{Cu—O})$ -19
	$A_g$		64		73 (0.1)	$\delta_1(\text{O—Cu—OH}_2)$ -47
$E_u$		74		71 (0.1)		$\tau(\text{Cu—O—C—C})$ -17 + $\tau(\text{R—R}')$ -16
$B_{2g}$			64		69	$\tau(\text{Cu—O—C—C})$ -22 + $\delta(\text{R—R}')$ -15
$E_u$		74		67		$\tau(\text{Cu—O—C—C})$ -35 + $\tau(\text{R—R}')$ -39 + $\tau_2(\text{R})$ -13
$E_g$			46		65 (0.1)	$\delta_2(\text{O—Cu—OH}_2)$ -78 + $\delta_2(\text{R})$ -19
	$A_u$	56		61		$\delta_1(\text{O—Cu—OH}_2)$ -70
$B_{2u}$		40		44		$\nu(\text{Cu—O})$ -19 + $\delta_2(\text{R})$ -18 + $\delta_2(\text{O—Cu—OH}_2)$ -41
$A_{1u}$		n.o.		10		$\tau_1(\text{R})$ -99

<sup>a</sup>  $\nu$ , Stretching;  $\delta$ , in-plane bending;  $\tau$ , out-of-plane bending; R, Cu—O—C—O—Cu ring.<sup>b</sup> n.o., Not observed<sup>c</sup> Downshifts upon  $^{63}\text{Cu}$ – $^{65}\text{Cu}$  substitution.

Among eight  $\nu(\text{Cu—O})$  vibrations expected, these approximated as the  $E_u$  species, show the largest isotope shift. Since normal frequencies were calculated for the molecule slightly deviated from  $D_{4h}$  symmetry, the discussed doubly degenerated  $E_u$  mode has two, 344 and 341 wavenumbers. The magni-

tude of calculated and observed  $^{63}\text{Cu}$ – $^{65}\text{Cu}$  displacements allow for unambiguous attribution of 376 and 331  $\text{cm}^{-1}$  bands to recently mentioned normal vibrations. The 45  $\text{cm}^{-1}$  difference corresponds well to structural data. As results from the X-ray measurements, in copper(II) acetate monohydrate,

a pair of opposite carboxylate groups form the Cu–O bonds about 0.04 Å longer than the remaining ones. These carboxylate oxygen atoms are also involved in hydrogen bonding with water molecules. Both effects may cause the mentioned 45 cm<sup>-1</sup> splitting of the  $\nu(\text{Cu–O})$  vibrations approximated here by E<sub>u</sub> species. The second IR active  $\nu(\text{Cu–O})$  mode (A<sub>2u</sub>) was predicted at 113 cm<sup>-1</sup> with 0.6 cm<sup>-1</sup> isotope shift. A 114 cm<sup>-1</sup> band of comparable intensity and isotope sensitivity has been proposed for that vibration.

The most intense Raman band of low frequency region was calculated at 279 cm<sup>-1</sup> as due to totally symmetric A<sub>1g</sub> vibration. Its observed position (323 cm<sup>-1</sup>) is 44 cm<sup>-1</sup> higher than that calculated, which again is due to mentioned differences in real Cu–O bonds. Other Raman active  $\nu(\text{Cu–O})$  modes described by E<sub>g</sub> species were computed at 247 and 233 cm<sup>-1</sup> and correlated with similar energy and intensity bands at 253 and 232 cm<sup>-1</sup>. The last  $\nu(\text{Cu–O})$  transition of B<sub>1g</sub> symmetry has been predicted as medium intensity band at 215 cm<sup>-1</sup>, strongly overlapping with  $\nu(\text{Cu–OH}_2)$  vibration at 216 cm<sup>-1</sup>. Both vibrations were attributed to 232 cm<sup>-1</sup> Raman band and its shoulder at 224 cm<sup>-1</sup>. The only inactive  $\nu(\text{Cu–O})$  vibration (B<sub>2u</sub>) is strongly coupled with other vibrations of the same symmetry and with O–Cu–OH<sub>2</sub> bending modes.

Special attention is usually focused on the Cu···Cu interaction. In the present calculations, the corresponding stretching  $\nu(\text{Cu–Cu})$  coordinate has been defined in order to get some recognition about the frequency of the motion where Cu···Cu distance is the most changed. It should be pointed out that this coordinate, corresponding frequency and force constant do not have to be related to chemical Cu–Cu bond. It is also possible to describe the discussed vibration as totally symmetric O–Cu–O bending mode, but this in turn, causes much more complicated description of eight-membered Cu–O–C–O–Cu–O–C–O ring deformations. In present work, the  $\nu(\text{Cu–Cu})$  stretching coordinate contributes mainly in 168 cm<sup>-1</sup> normal A<sub>1g</sub> vibration exhibiting 1.2 cm<sup>-1</sup> metal isotope shift. Based on the calculated frequency and strongly on the isotope shift, the discussed mode has been attributed to 178 cm<sup>-1</sup> Raman band showing 2.0 cm<sup>-1</sup> displacement upon <sup>63</sup>Cu–<sup>65</sup>Cu substitution.

The Cu–Cu–O bending vibrations are mainly represented by  $\delta_2(\text{R})$  Cu–O–C–O–Cu ring deformation. As expected, these vibrations are more coupled with other modes. The highest PED percentages of  $\delta_2(\text{R})$  were calculated for 103, 99 and 241 cm<sup>-1</sup> normal vibrations of E<sub>g</sub> and A<sub>2u</sub> symmetry, respectively. Third, B<sub>2u</sub> mode is dispersed over three vibrations with the highest contribution (40%) in the 153 cm<sup>-1</sup> transition.

The torsional deformation of the O–Cu···Cu–O subunit is implemented in the  $\tau_1(\text{R})$  coordinate. The calculations show, that all corresponding vibrations should produce very weak bands – more than twenty times weaker than in, e.g., the 279 cm<sup>-1</sup> Raman band and 344, 341 cm<sup>-1</sup> IR absorptions. Thus, a small shoulder at 210 cm<sup>-1</sup> in Raman spectrum has been proposed for E<sub>g</sub> type vibrations predicted at 207 and 197 cm<sup>-1</sup>.

To complete the vibrations in which the copper atoms are involved, the inter-ring bending and torsion modes have to be considered. In Table 2, these vibrations were labeled as  $\delta(\text{R–R}')$  and  $\tau(\text{R–R}')$ , respectively. The Raman active  $\delta(\text{R–R}')$  mode (B<sub>2g</sub>) contributes significantly in 228 cm<sup>-1</sup> vibration and has been attributed to 232 cm<sup>-1</sup> band together with previously discussed  $\nu(\text{Cu–O})$  of E<sub>g</sub> symmetry. The degenerate  $\tau(\text{R–R}')$  mode (E<sub>u</sub>) is dispersed over four normal vibrations and coupled with  $\tau(\text{Cu–O–C–C})$  deformation. The highest PED term of  $\tau(\text{R–R}')$  coordinate has been found in 221, 220 cm<sup>-1</sup> degenerate vibration, assigned to more split absorption maxima at 253 and 234 cm<sup>-1</sup>.

Since calculations were carried out for whole [Cu<sub>2</sub>(OOCCH<sub>3</sub>)<sub>4</sub>(H<sub>2</sub>O)<sub>2</sub>] molecule, it was possible to evaluate the vibrations related to water groups. In order to provide an additional proof of computation results, the IR spectrum of the complex substituted with D<sub>2</sub>O was measured and computed. In calculations, the stretching Cu–OH<sub>2</sub> modes are predominant in three normal vibrations. The highest frequency mode with significant contribution of  $\nu(\text{Cu–OH}_2)$  is predicted at 256 cm<sup>-1</sup> as a very weak Raman transition with an H–D shift below 1 cm<sup>-1</sup>. In theoretical Raman spectrum this mode is overlapped by about six times more intense vibration at 247 cm<sup>-1</sup>, thus it will be difficult to observe the former mode. Two remaining IR active vibrations computed at 223 and 216 cm<sup>-1</sup> are also weak and positioned close to much more intense 221 cm<sup>-1</sup> band. Upon deuteration, the first vibration remains unchanged, whereas the second vibration shifts to 212 cm<sup>-1</sup>. Since the IR bands observed between 400 and 180 cm<sup>-1</sup> are not sensitive to H<sub>2</sub>O–D<sub>2</sub>O replacement, the recently mentioned Cu–OH<sub>2</sub> vibrations should be considered as unobservable. The only observed deuteration effect in the far-IR spectrum is the disappearance of the 175 cm<sup>-1</sup> shoulder, which may be correlated with twisting mode of H<sub>2</sub>O groups calculated at 190 cm<sup>-1</sup>. The main band at 182 cm<sup>-1</sup> is probably due to lattice vibrations which may also generate some other weak absorptions below 150 cm<sup>-1</sup>, not attributed so far to molecular transitions. The contribution of lattice modes is also possible for relatively intense Raman bands located in the same frequency region.

### 3.2. Middle-IR region

The bands observed in the middle-IR region between 1800 and 600 cm<sup>-1</sup> may be classified into three groups: the skeletal modes of CH<sub>3</sub>–COO groups, the C–H deformations and bending vibrations of water molecules. The last absorption has been easily located as the 1650 cm<sup>-1</sup> shoulder, which disappears upon H<sub>2</sub>O–D<sub>2</sub>O replacement with simultaneous appearance of new 1213 cm<sup>-1</sup> band due to  $\delta(\text{D}_2\text{O})$  vibration. As has been presented in Fig. 4, very similar effect results from calculations.

The expected eight  $\nu(\text{C–O})$  vibrations (with two doubly degenerated) are well separated into symmetric and anti-symmetric modes with respect to local COO group

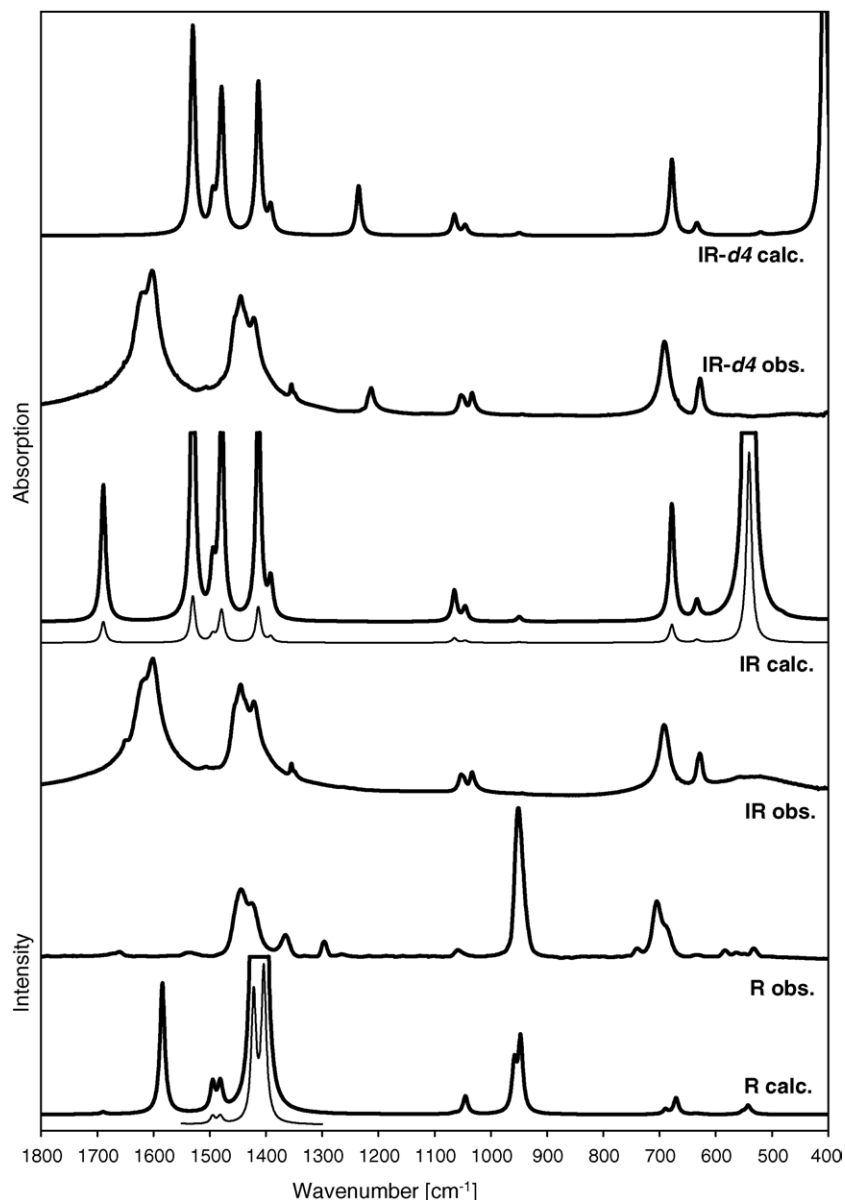


Fig. 4. Observed and DFT calculated spectra in middle-IR region.

symmetry or  $\sigma_h$  plane of  $D_{4h}$  symmetry used here. The anti-symmetric vibrations are observed in the IR spectrum as intense band with maximum at  $1605\text{ cm}^{-1}$  and shoulder at about  $1620\text{ cm}^{-1}$ . The corresponding normal vibrations were computed at  $1530\text{ (A}_{2u}\text{)}$  and  $1551\text{ cm}^{-1}\text{ (B}_{2u}\text{)}$  as very intense and weak transitions, respectively. Third anti-symmetric mode ( $E_g$ ) was computed at  $1584\text{ cm}^{-1}$ , but the only candidate for this mode is the weak Raman band at  $1535\text{ cm}^{-1}$  (higher frequency band is probably due to  $\delta(\text{H}_2\text{O})$  vibrations). The symmetric  $\nu(\text{C-O})$  vibrations are less separated and has been calculated at  $1422\text{ (A}_{1g}\text{)}$  and  $1404\text{ cm}^{-1}\text{ (B}_{1g}\text{)}$ . These two strong Raman transitions have been correlated with two bands at  $1444$  and  $1426\text{ cm}^{-1}$ , being the most intense in the discussed area. However, these two bands are probably also generated by  $\delta(\text{CH}_3)$  vibrations calculated

between  $1470$  and  $1500\text{ cm}^{-1}$ , but their predicted low intensity suggests that discussed bands are mainly due to  $\nu(\text{C-O})$  vibrations. Similar phenomenon is observed in the IR spectrum, but according to calculations, the  $\delta(\text{CH}_3)$  vibrations have the intensities similar to that of  $\nu(\text{C-O})$  at  $1414\text{ cm}^{-1}\text{ (E}_u\text{)}$ . Thus, the absorption maximum at  $1421\text{ cm}^{-1}$  has been proposed for  $\nu(\text{C-O})$  mode, whereas the  $1445\text{ cm}^{-1}$  peak assigned to  $\delta(\text{CH}_3)$  vibrations.

The recently presented  $\nu(\text{C-O})$  vibrations are coupled with the  $\nu(\text{C-C})$  modes, calculated mainly at close positions around  $950\text{ cm}^{-1}$ . Two of these vibrations at  $958$  and  $947\text{ cm}^{-1}$  are Raman active and may be correlated with the intense band, observed at  $951\text{ cm}^{-1}$ . The IR active ( $E_u$ ) mode is predicted as  $950\text{ cm}^{-1}$  band of very low intensity, comparable with very weak absorption observed at  $944\text{ cm}^{-1}$ .

The 700–600  $\text{cm}^{-1}$  part of the middle-IR area is occupied by “in plane”  $\delta_1(\text{R})$  and “out-of-plane”  $\tau_2(\text{R})$  deformations of bridging rings in which the motions of carboxylate carbon atoms are predominant. As results from the respective IR spectra (Fig. 4), for both  $E_u$  deformations the bands computed at 678 and 633  $\text{cm}^{-1}$  correspond very well to those observed at 692 and 629  $\text{cm}^{-1}$ . Raman transitions are a little more complicated, because four calculated transitions have different intensities:  $B_{1g}$  mode at 671  $\text{cm}^{-1}$  is medium intensity,  $A_{1g}$  (689  $\text{cm}^{-1}$ ) and  $B_{2g}$  (637  $\text{cm}^{-1}$ ) are weak, whereas the  $A_{2g}$  (623  $\text{cm}^{-1}$ ) is very weak. Following these relative intensities, the most intense band at 706  $\text{cm}^{-1}$  has been proposed for  $B_{1g}$  mode and band at 692  $\text{cm}^{-1}$  for  $A_{1g}$  species. Among two Raman active  $\tau_2(\text{R})$  transitions, only the  $B_{2g}$  was recorded at 635  $\text{cm}^{-1}$ .

In the frequency range between 600 and 400  $\text{cm}^{-1}$ , two kinds of vibrations were predicted and observed: the  $\delta(\text{O}-\text{C}-\text{C})$  bending and water motions. Only one of the former vibrations was observed in the Raman spectrum. In the IR spectrum, this region is mostly covered by broad band with maximum about 550  $\text{cm}^{-1}$  exhibiting about 90  $\text{cm}^{-1}$  downshift upon deuteration. This effect is well reproduced in calculations where intense band generated by wagging (552  $\text{cm}^{-1}$ ) and rocking (547  $\text{cm}^{-1}$ ) vibrations of water molecules is shifted to 405  $\text{cm}^{-1}$  by H-D replacement.

The remaining bands of discussed middle-IR region are related to  $\text{CH}_3$  group vibrations. Vibrations of these groups also cover the highest frequency area together with intense and well separated  $\text{H}_2\text{O}$  stretching vibrations at 3475 and 3375  $\text{cm}^{-1}$ , shifted to 2590 and 2490  $\text{cm}^{-1}$  upon deuteration.

#### 4. Conclusions

Vibrational spectra of  $[\text{Cu}_2(\text{OOCCH}_3)_4(\text{H}_2\text{O})_2]$  complex have been measured and interpreted with help of deuteration and metal isotope experiments as well as theoretical calculations (DFT) reproducing the spectra and mentioned isotope labeling effects.

Following the observation that the symmetry of  $[\text{Cu}_2\text{O}_8\text{C}_4]$  core only slightly deviate from  $D_{4h}$  point group, it has been demonstrated that normal vibrations of this structural unit can be effectively presented using the internal coordinates of  $D_{4h}$  symmetry. Such an approximation allows for simple and clear description of most important normal vibrations related to  $\text{Cu}-\text{Cu}$ ,  $\text{Cu}-\text{O}$ ,  $\text{C}-\text{O}$  and  $\text{C}-\text{C}$  stretching coordinates and some deformation modes.

Side effects resulting from applied  $D_{4h}$  approximation (frequency splitting of some degenerated vibrations, very weak activity of selected forbidden transitions) appeared to be not disturbing the interpretation of observed fundamentals.

The most intense copper–oxygen stretching vibrations were attributed to 376, 331, 114  $\text{cm}^{-1}$  IR absorptions and 323, 224  $\text{cm}^{-1}$  Raman transitions. One of the most interesting mode related to elongation of  $\text{Cu}\cdots\text{Cu}$  distance was calculated at 168  $\text{cm}^{-1}$  and assigned to 178  $\text{cm}^{-1}$  Raman band exhibiting the 2.0  $\text{cm}^{-1}$  isotope shift.

#### Acknowledgements

Thanks are due to Poznań Supercomputing Centre for computation facilities and to Tomasz Miasaszek for help in Raman measurements.

#### References

- [1] J. Catteric, P. Thornton, *Adv. Inorg. Chem. Radiochem.* 20 (1977) 291.
- [2] A.B.P. Lever, B.S. Ramaswamy, *Can. J. Chem.* 51 (1973) 514.
- [3] J.A. Faniran, K.S. Patel, *J. Inorg. Nucl. Chem.* 36 (1974) 2261.
- [4] L.P. Battaglia, A. Bonamartini Corradi, G. Marcotrigiano, L. Menabue, G.C. Pellacani, *Inorg. Chem.* 20 (1981) 1075.
- [5] P. Baraldi, G. Fabbri, *Spectrochim. Acta* 37A (1981) 89.
- [6] J. San Filippo Jr., H.J. Sniadoch, *Inorg. Chem.* 12 (1973) 2326.
- [7] G.A. Schick, D.F. Bocian, *J. Raman Spectrosc.* 11 (1981) 27.
- [8] M.J. Frisch, G.W. Trucks, H.B. Schlegel, G.E. Scuseria, M.A. Robb, J.R. Cheeseman, V.G. Zakrzewski, J.A. Montgomery Jr., R.E. Stratmann, J.C. Burant, S. Dapprich, J.M. Millam, A.D. Daniels, K.N. Kudin, M.C. Strain, O. Farkas, J. Tomasi, V. Barone, M. Cossi, R. Cammi, B. Mennucci, C. Pomelli, C. Adamo, S. Clifford, J. Ochterski, G.A. Petersson, P. Y. Ayala, Q. Cui, K. Morokuma, D. K. Malick, A. D. Rabuck, K. Raghavachari, J.B. Foresman, J. Cioslowski, J.V. Ortiz, A.G. Baboul, B.B. Stefanov, G. Liu, A. Liashenko, P. Piskorz, I. Komaromi, R. Gomperts, R.L. Martin, D.J. Fox, T. Keith, M.A. Al-Laham, C.Y. Peng, A. Nanayakkara, M. Challacombe, P.M.W. Gill, B. Johnson, W. Chen, M.W. Wong, J. L. Andres, C. Gonzalez, M. Head-Gordon, E.S. Replogle, J.A. Pople, *Gaussian 98, Revision A.9*, Gaussian Inc., Pittsburgh, PA, 1998.
- [9] A.D. Becke, *J. Chem. Phys.* 104 (1996) 1040.
- [10] P.J. Hay, W.R. Wadt, *J. Chem. Phys.* 82 (1985) 270.
- [11] T.H. Dunning Jr., P.J. Hay, *Modern Theoretical Chemistry*, Plenum Press, New York, 1976.
- [12] L. Lapinski, M.J. Nowak, Balga—computer program for PED calculation.
- [13] G. Schaftenaar, J.H. Noordik, Molden: a pre- and post-processing program for molecular and electronic structures, *J. Comput. Aided Mol. Des.* 14 (2000) 123.
- [14] M.M. Szczesniak, B. Maslanka, AniMol—computer program Infrared and Raman Spectroscopy Teaching Tool, Ver. 3. 21, 1997.
- [15] M.H. Brooker, O. Faursov Nielsen, E. Praestgaard, *J. Raman Spectrosc.* 19 (1988) 71.
- [16] P. Drożdżewski, B. Pawlak, *Vibrat. Spectrosc.* 33 (2003) 15.
- [17] P. de Meester, S.R. Fletcher, A.C. Skapski, *J. Chem. Soc., Dalton Trans.* 23 (1973) 2575.
- [18] G.M. Brown, R. Chidambaram, *Acta Cryst.* 29B (1973) 2393.
- [19] P. Pulay, G. Fogarasi, F. Pang, J.E. Boggs, *J. Am. Chem. Soc.* 10 (1979) 2550.